

# Optimization of Methanol Steam Reforming Reactor with Variable Cross-Sectional Based on Reaction Characteristics

JIANG Xinyu<sup>1</sup>, HE Zhenzong<sup>1,2\*</sup>, MAO Junkui<sup>1</sup>, ZHU Ruihan<sup>1</sup>, RAN Qianxi<sup>1</sup>

1. College of Energy and Power Engineering, Nanjing University of Aeronautics and Astronautics, Nanjing 210016, P. R. China; 2. Collaborative Innovation Center for Advanced Aero-Engine, Beijing 100191, P. R. China

(Received 10 May 2023; revised 13 July 2023; accepted 20 August 2023)

**Abstract:** The flow field characteristics in the reforming channel and the temperature distribution characteristics of the catalytic bed under the hot air heating condition are first investigated in a double-jacketed methanol steam reforming (MSR) reactor. It is shown that the temperature of the catalytic bed decreases rapidly along the flow direction, with the minimum temperature region at 15 mm to 20 mm from the catalytic bed inlet. And the temperature increases gradually with the flow direction to approach the heating temperature. In addition, the temperature gradually increases along the radius from the center to the wall, and heat transfer resistance makes the temperature in the middle of the catalyst bed lower than the temperature around. Based on this reaction characteristic, a variable cross-sectional reforming reactor is proposed in this paper to completely utilize the heat supply energy and improve the reaction efficiency. The response surface methodology (RSM) is then used to optimize the structural parameters of the variable cross-section reactor. It is shown that the methanol conversion is significantly increased at the same boundary conditions for the outer radius  $R_1=49.94$  mm at the reforming inlet of the heating channel, the radius  $R_2=39.99$  mm at the minimum cross-section and the distance  $D=98.44$  mm from the minimum cross-section to the catalytic bed inlet.

**Key words:** methanol steam reforming; variable cross-sectional reactor; methanol conversion; response surface methodology

**CLC number:** TK123

**Document code:** A

**Article ID:** 1005-1120(2023)S2-0094-09

## 0 Introduction

Hydrogen is an important secondary energy source in the core conversion position in multiple energy systems. It is considered the best alternative to traditional fossil fuel (e.g., domestic RP-3 aviation kerosene) because of its high calorific value, zero emissions and no pollution, and its application in aerospace and other fields has received wide attention from domestic and foreign research institutions and aero-engine manufacturers<sup>[1-2]</sup>. Despite many advantages as a clean energy source, hydrogen has challenges in storage and transportation. Storage and transportation technology are key factors restricting hydrogen efficient development and utilization. Therefore, direct hydrogen production technol-

ogy has received attention to meet the hydrogen demand in modern society instead of its storage and transportation.

With the advantages such as easy availability, easy storage, low toxicity, low reaction temperature for hydrogen production, high hydrogen-carbon ratio, and no sulfur, methanol has been defined as competitive material for hydrogen production<sup>[3-5]</sup>. The reforming reactor is a key device for converting methanol to hydrogen, and its design is crucial to improve the efficiency of methanol steam reforming to hydrogen. Therefore, it is of great significance in engineering applications to improve the reaction efficiency of methanol-reforming hydrogen production by establishing the structural model of micro metha-

\*Corresponding author, E-mail address: hezhenzong@nuaa.edu.cn.

**How to cite this article:** JIANG Xinyu, HE Zhenzong, MAO Junkui, et al. Optimization of methanol steam reforming reactor with variable cross-sectional based on reaction characteristics [J]. Transactions of Nanjing University of Aeronautics and Astronautics, 2023, 40(S2): 94-102.

<http://dx.doi.org/10.16356/j.1005-1120.2023.S2.013>

nol steam reforming reactor, analyzing the influence of reactor structure on the performance of methanol-reforming hydrogen production, and then studying the characteristics of different structures to improve the reforming characteristics and optimize structural parameters.

According to Ref. [6], microchannels can be generally classified into two major types: ordered microchannels (for substrate materials) and 3D network microchannels (for porous materials). Numerous numerical and experimental studies regarding the structural design of ordered microchannel reformers have sprung up in the 21st century. Ribeirinha et al.<sup>[7]</sup> proposed the combination of a high-temperature proton exchange membrane fuel cell (PEMFC) with a methanol steam reformer after numerical simulation. Both the fuel cell and the reforming chamber use the serpentine direct microchannel, in which the reactions of methanol steam reforming (MSR), reverse water gas shift (RWGS), and methanol decomposition (MD) were considered in their calculation. The poisoning effect of CO on the electro-catalytic activity of the membrane electrode assembly (MEA) was also evaluated. As a result, both the rise of the space-time ratio and the reforming temperature can increase CO concentration. Mei et al.<sup>[8]</sup> studied an A-type microchannel reactor with a flow pattern of one inlet and two outlets to optimize the traditional Z-type design. With a combination of simulation and experiments, the component distributions in the A-type microchannel reactor were found to be more homogeneous than those in the Z-type one. Although researchers had paid much attention to developing new microchannels with various structures, relatively few scholars had paid attention to improving reactor structure based on reaction characteristics.

The objective of this study is to comparatively analyze the reaction characteristics of MSR reaction by CFD simulation and further obtain the optimal structure of the microchannel and the structural parameters of the variable cross-section reactor, which are optimized by response surface methodology (RSM) to achieve high methanol conversion and high hydrogen production.

## 1 Physical, Mathematical and Kinetic Models

### 1.1 Physical model

The schematic diagram and cross-sectional dimensions of the overall structure of the double-jacketed tubular reforming reactor used in this paper are shown in Fig.1. The hot air provided by the external heat source enters the heating channel from the inlet to supply heat to the reforming reaction. The mixture of methanol and water enters the reaction channel through the reactant inlet. The geometrical parameters of the reactor are shown in Table 1.

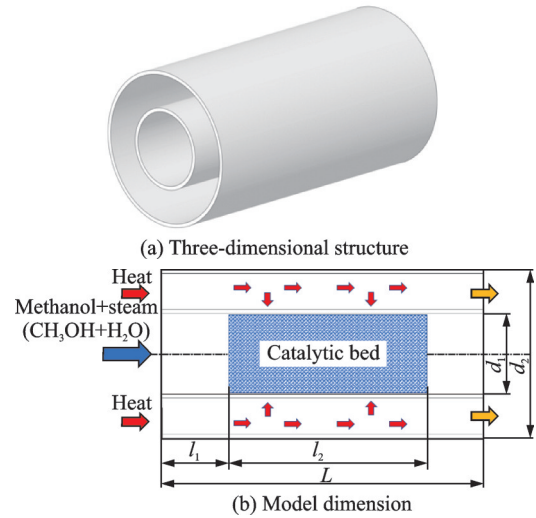


Fig.1 Schematic diagram of restructuring reactor structure

**Table 1 Geometrical parameters of reforming reactor**

Parameter	Value
Reforming reactor length $L$ / mm	160
Ingress segment length $l_1$ / mm	30
Catalytic bed length $l_2$ / mm	100
Reforming gas channel diameter $d_1$ / mm	40
Hot air channel diameter $d_2$ / mm	80
Wall thickness / mm	2

### 1.2 Control equation

Continuity equation is shown as

$$\nabla \cdot \mathbf{V} = 0 \quad (1)$$

Momentum equation is shown as

$$\varepsilon (\mathbf{V} \cdot \nabla) \mathbf{V} = -\frac{\varepsilon_0}{\rho_f} \nabla p + \frac{\varepsilon_0 \mu}{\rho_f} \nabla^2 \mathbf{V} + S_m \quad (2)$$

where  $\varepsilon$  is the catalyst porosity and set as  $0.5^{[9]}$ ,  $\rho_f$  the density of the fluid,  $\mu$  the viscosity of the mixture, and  $S_m$  the momentum source term generated

by the porous catalyst, shown as

$$S_m = -\frac{\mu}{\rho_f K} \mathbf{V} - \frac{\beta \mathbf{V}}{2} |\mathbf{V}| \quad (3)$$

where  $K$  is the permeability, and  $\beta$  the inertia loss coefficient in each direction in the porous material of the catalyst.

Component concentration equation is shown as

$$\varepsilon (\mathbf{V} \cdot \nabla) C_i = D_{\text{eff}} \nabla^2 C_i + \varepsilon \sum_{r=1}^N M_{w,i} R_{i,r} \quad (4)$$

where  $C_i$  denotes the concentration of the  $i$ th substance  $\text{CH}_3\text{OH}$ ,  $\text{H}_2\text{O}$ ,  $\text{H}_2$ ,  $\text{CO}_2$ , and  $\text{CO}$ ,  $D_{\text{eff}}$  the effective mass diffusion coefficient based on the Stefan-Maxwell equation,  $M_{w,i}$  the molecular weight of the  $i$ th species,  $R_{i,r}$  the reaction rate of reaction  $r$ , and the last term is the source term of the chemical reaction induced in the catalyst. For the non-catalyst region, this term is zero.

Energy equation is shown as

$$(\rho_f c_p) (\mathbf{V} \cdot \nabla) T = \lambda_{\text{eff}} \nabla^2 T + \varepsilon S_t \quad (5)$$

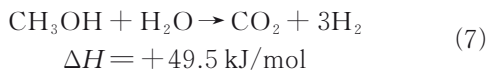
where  $\lambda_{\text{eff}}$  is the effective thermal conductivity;  $T$  represents the temperature; and the source term  $S_t$  in the energy equation, caused due to the chemical reaction, is zero in the reactor except for the catalyst region. It can be expressed as

$$\lambda_{\text{eff}} = \varepsilon \lambda_f + (1 - \varepsilon) \lambda_s \quad (6)$$

where  $\lambda_f$  and  $\lambda_s$  are the fluid thermal conductivity and solid thermal conductivity in porous media, respectively.

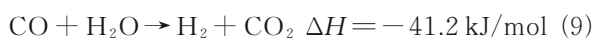
With regard to the chemical reaction equations, Srivastava et al.<sup>[10]</sup> showed that the methanol steam reforming reaction occurs faster than the steam conversion reaction. Therefore, the following reaction process was applied in this study.

(1) Methanol steam reforming reaction



where  $\Delta H$  represents the amount of heat released or absorbed by the chemical reaction.

(2) Water gas shift reaction



The Arrhenius model is used to calculate the rates of the above chemical reactions. The rate expressions for the methanol MSR  $R_{\text{MSR}}$  and the re-

verse water gas shift (rWGS)  $R_{\text{rWGS}}$  are

$$R_{\text{MSR}} = k_1 C_{\text{CH}_3\text{OH}}^{0.6} C_{\text{H}_2\text{O}}^{0.4} \exp\left(-\frac{E_{a_1}}{RT}\right) \quad (10)$$

$$R_{\text{rWGS}} = k_2 C_{\text{CO}_2} C_{\text{H}_2} \exp\left(-\frac{E_{a_2}}{RT}\right) - k_{-2} C_{\text{CO}} C_{\text{H}_2\text{O}} \exp\left(-\frac{E_{a_2}}{RT}\right) \quad (11)$$

where  $k$  is the pre-exponential factor and  $E_a$  the activation energy corresponding to the reaction. The relevant parameters are shown in Table 2<sup>[10-11]</sup>.

**Table 2 Basic parameters used in this study**

Parameter	Value
Density of catalyst bed $\rho$ / ( $\text{kg}\cdot\text{m}^{-3}$ )	1 480
Thermal conductivity of solid catalyst $\lambda_s$ / ( $\text{W}\cdot\text{m}^{-1}\cdot\text{K}^{-1}$ )	1
Catalyst bed porosity $\varepsilon$	0.5
Mass diffusion coefficient $D_k$ / ( $\text{m}^2\cdot\text{s}^{-1}$ )	$6.8 \times 10^{-5}$
Universal gas constant $R$ / ( $\text{J}\cdot\text{mol}^{-1}\cdot\text{K}^{-1}$ )	8 314
Pre-exponential factor for steam reforming $k_1$ / $\text{s}^{-1}$	$8 \times 10^8$
Pre-exponential factor for reverse WGS $k_2$ / ( $\text{m}^3\cdot\text{mol}^{-1}\cdot\text{s}$ )	$4 \times 10^8$
Pre-exponential factor for backward WGS $k_{-2}$ / ( $\text{m}^3\cdot\text{mol}^{-1}\cdot\text{s}$ )	$4 \times 10^8$
Activation energy for steam reforming $E_{a_1}$ / ( $\text{J}\cdot\text{mol}^{-1}$ )	$7 \times 10^7$
Activation energy for reverse WGS $E_{a_2}$ / ( $\text{J}\cdot\text{mol}^{-1}$ )	$1 \times 10^8$
Activation energy for backward WGS $E_{a_{-2}}$ / ( $\text{J}\cdot\text{mol}^{-1}$ )	$1 \times 10^8$

The methanol conversion can be obtained from Eq.(12).

$$X_{\text{CH}_3\text{OH}} = \frac{C_{\text{CH}_3\text{OH},\text{in}} - C_{\text{CH}_3\text{OH},\text{out}}}{C_{\text{CH}_3\text{OH},\text{in}}} \times 100\% \quad (12)$$

where  $C_{\text{CH}_3\text{OH},\text{in}}$  and  $C_{\text{CH}_3\text{OH},\text{out}}$  denote the mass fraction of methanol at inlet and outlet, respectively.

### 1.3 Boundary conditions

The calculation parameters used in the simulation are listed in Table 3.

### 1.4 Grid independence analysis and numerical model validation

The numerical calculation results are shown in Fig.2, when the number of grids is 39 156, 135 366, 201 405, 421 716, 581 742, and 736 230, respectively. When the grids are 581 742, the numerical calculation results almost no longer show significant

**Table 3** Calculation parameters used in simulation

Parameter	Value
Hot air inlet speed / ( $\text{m}\cdot\text{s}^{-1}$ )	0.5—3.0
Hot air inlet temperature / K	523—673
Reactant speed / ( $\text{m}\cdot\text{s}^{-1}$ )	0.1
Reactant inlet temperature / K	453
Steam-carbon ratio	1.1
Porosity	0.5
Outlet pressure / MPa	0.1

changes as the mesh increases. Considering the accuracy and high efficiency of the calculation, 581 742 grids are chosen to carry out the subsequent research work.

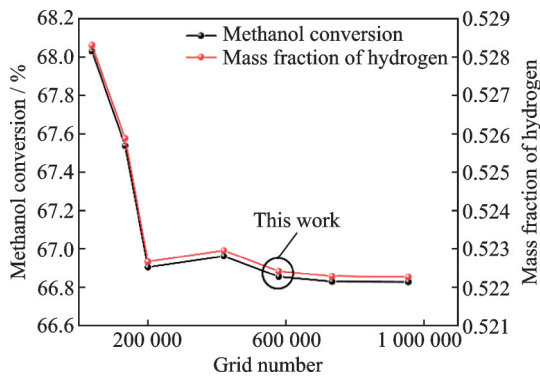
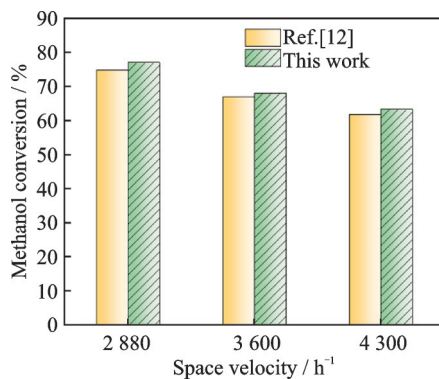


Fig.2 Grid independent verification

To ensure the validity of the model, the simulation results are compared with the experimental data performed by Fukahori et al.<sup>[12]</sup>. As shown in Fig.3, the methanol conversion obtained by comparing the simulation of this model is 89.81%, 76.93%, and 61.32% at the space velocity of 1 075, 2 150, and 4 300  $\text{h}^{-1}$ , respectively. And the difference between the simulation results and the experimental data in Ref.[12] is within 3%, which fully proves the accuracy of the numerical model in this paper.

Fig.3 Validation of the numerical model<sup>[12]</sup>

## 2 Results and Discussion

### 2.1 Characteristic of methanol steam reforming in a double-jacketed reformer reactor

From the temperature distribution in Fig.4, the fuel mixture is preheated and reformed in the catalyt-

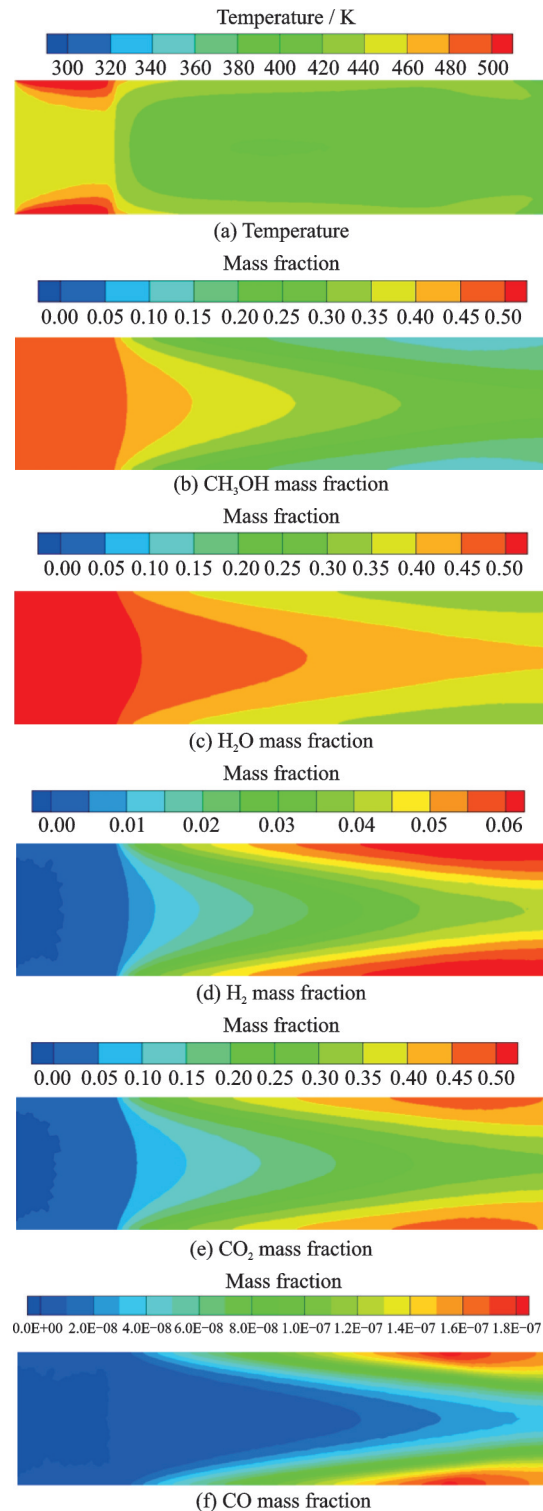


Fig.4 Temperature and component distribution of the double-jacketed reforming reactor

ic bed. As the reaction absorbs heat, the catalytic bed temperature decreases significantly. The trends in the mass fractions of products such as hydrogen and carbon dioxide are opposite to that of the methanol and steam mass fractions. This phenomenon is because, at the beginning of the methanol and steam mixture entering the catalytic bed, the MSR reforming reaction is rapidly carried out under the action of the catalyst, the methanol consumption increases sharply, and the content of hydrogen and carbon dioxide increases rapidly<sup>[13]</sup>. It is obvious that the MSR reaction is reversible and will eventually reach chemical equilibrium as the reaction proceeds. From the distribution of each component in Fig.4, it can also be found that the reaction is more intense at the catalytic bed wall, and the molar concentrations of methanol and steam gradually decrease along the reactor radial direction from the center. In contrast, the molar concentrations of products such as hydrogen and carbon dioxide show the opposite trend. This is since the heat flow density is higher near the wall, and the reaction is stronger. While the thermal resistance is higher at the center of the reactor, and the reaction rate is slightly lower than that at the wall.

The temperature distribution in the catalytic bed is shown in Fig.5. From the trend of temperature change in Fig.5, and it can be seen that the temperature along the flow direction drops rapidly from 441.26 K at the inlet of the catalytic bed to 409.2 K at the end of the catalytic bed. Besides, the temperature gradually decreases from the wall to the center

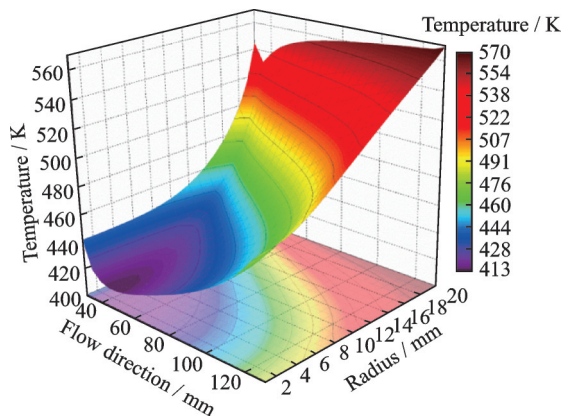


Fig.5 Diagram of the flow field in heating channel of the non-ribbed double-jacketed reforming reactor

along the radius. In addition, from the radius direction of the inlet cross-sectional, the temperature gradually increases from the center along the radius direction. As the reaction proceeds, the catalytic bed section is fully heated, the concentration of reactants gradually decreases, and the temperature gradually increases.

## 2.2 Variable cross-sectional methanol steam reforming reactor based on reaction characteristics

According to the temperature distribution characteristics of the catalytic bed above, the preliminary scheme for enhancing the heating capacity of the reactor based on the reaction characteristics can be summarized as follows: In the rapid reaction zone of contact with the catalytic bed, the heating channel adopts a reducing section. The reduced section is used in the violent reaction section, and it can be seen from the Bernoulli equation that the hot air flow velocity gradually increases and the heat flux density gradually increases due to the gradual shrinkage of the section, so the heating capacity in the reforming channel is strengthened. However, the gentle reaction zone in the catalytic bed adopts a gradual divergent section. Because the flow velocity is not supersonic, the hot air is affected by the gradual expansion of the section, and the flow velocity gradually decreases, which ensures that the hot air is fully in contact with the reforming channel and provides heat for the reforming reaction. As shown in Fig.6, the cross-sectional characteristics of the reactor are summarized as the outer radius of the hot air channel  $R_1$ , the minimum interface outer radius  $R_2$ , and the distance  $D$  of the two sections.

The shape of the cross-section is determined by the radius  $R_1$  at the reforming inlet, the radius  $R_2$  at

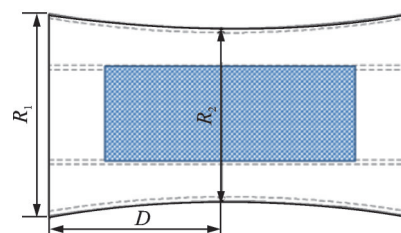


Fig.6 The geometry of variable cross-sectional heating channel reforming reactor

the minimum cross-section and the axial distance  $D$  from the front to the minimum cross-section. The flow field distribution during the reforming reaction is shown in Fig.4. When the reforming gas is in contact with the catalyst bed, the heating channel cross-section can be appropriately reduced to increase the local flow velocity, thus, the heating capacity. Meanwhile, it can be seen from the flow field distribution of the hot air channel in Fig.7 that the temperature of hot air in the channel drops significantly as the supply gas flows to the reforming channel for heating.

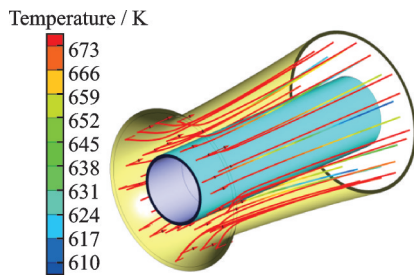


Fig.7 Diagram of flow field in heating channel of the double-jacketed reforming reactor

Compared with the original reactor for the hot air temperature range from 553 K to 673 K, the simulation results of the variable cross-section heating channel are shown in Fig.8. It can be seen that the methanol conversion of the variable cross-sectional reactor increases from 62.71% to 88.32% and is generally higher than that of the original reactor when the hot air temperature gradually increases. This indicates that the methanol conversion of the variable cross-sectional reactor is better than that of the original reactor when the inlet and outlet bound-

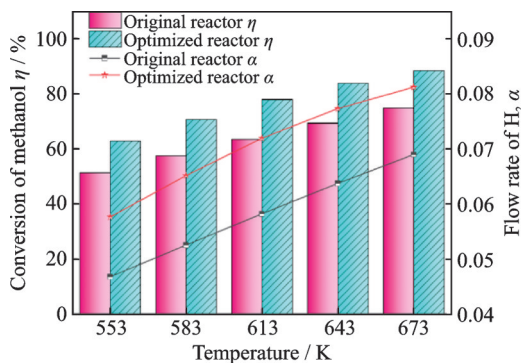


Fig.8 Reforming effect of variable cross-section reforming reactor

ary conditions are constant. It can be concluded that the reactor with variable cross-sectional heating channels has a better heating effect, and the reforming reaction occurs more fully under the same boundary conditions.

### 2.3 Optimization of variable cross-section methanol steam reforming reactor

From the previous study, it can be found that the variable cross-sectional reactor based on the reaction characteristics effectively enhances the heat transfer on the hot air side in the double-jacketed reforming reactor and improves the catalytic reforming efficiency of methanol. It is shown that the optimized design of the geometry of the variable cross-section heat supply channel helps further to improve the heat transfer performance of the reactor.

To further explore the optimal structure, the response surface methodology is adopted to optimize the design of heating channels in this paper to study the effects of  $R_1$ ,  $R_2$ ,  $D$  and other parameters on the characteristics of hydrogen production from methanol reforming in the reactor. And the methanol conversion and hydrogen flow rate are used as the evaluation indexes for the optimal design of the reactor. As a result, a database was established.

An analysis of variance (ANOVA) was performed on the model to assess the accuracy of the model. As shown in Table 4, the  $F$ -values for both methanol conversion and hydrogen flow responses are large and the  $P$ -values less than 0.000 1, indicating that the fitted model is highly statistically significant.  $R^2$  and Adj  $R^2$  are close to 1, the difference between Adj  $R^2$  and Pred  $R^2$  is less than 0.2, and C.V.% is less than 10, proving that the model is desirable. In addition, Fig.9 shows the predicted values of response surface analysis compared with the

Table 4 Variance analysis of methanol conversion and hydrogen flow rate

Response	Methanol conversion rate	Hydrogen flow
$F$ -value	20.87	33.23
$P$ -value	<0.000 1	<0.000 1
$R^2$	0.964 1	0.977 6
Adj $R^2$	0.917 9	0.948 7
Pred $R^2$	0.883 7	0.824 5
C.V.%	3.88	3.18

actual values of the numerical model. As seen from Fig.9, the predicted and actual values fit relatively closely, indicating that the model is very reliable in predicting the data.

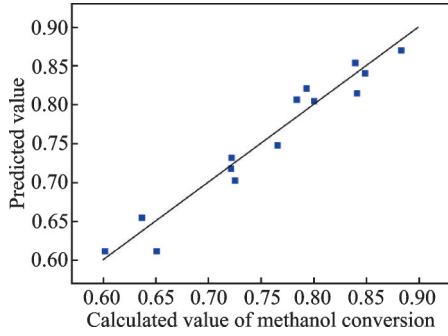


Fig.9 Comparison between calculated value and predicted value

From the above study, it is clear that  $R_1$ ,  $R_2$ , and  $D$  all have some influence on the reactor performance, and the influence mechanisms are different. For this reason, based on the CFD simulation results above, the response surface methodology is applied to optimize each parameter affecting the performance of the reformer reactor. The optimized parameters of the variable cross-sectional reactor structure are shown in Table 5 and Table 6. The optimized methanol conversion rate is 99.15%, and the hydrogen flow rate is 0.006 849 g/s. Meanwhile, it is shown that the relative error of methanol conversion and hydrogen flow rate is within 1%, which is within the acceptable range and fully demonstrates the reliability of the optimization model.

**Table 5 Optimal values of cross-section parameters obtained based on response surface optimization method** mm

Parameter	Optimization value
$R_1$	49.94
$R_2$	39.99
$D$	98.44

**Table 6 Optimization values based on response surface optimization method**

Response result	Optimization value
Methanol conversion(CFD calculation)/%	98.63
Methanol conversion rate (response surface prediction) / %	99.15
Hydrogen flow rate(CFD calculation)	0.006 513
Hydrogen flow rate(response surface prediction)	0.006 849

Fig.10 shows the temperature distribution comparison of the original and variable cross-section reactor under the same heating parameters. It can be seen that the hot air is more fully preheated in the inlet section when the heating channel adopts a variable cross-section, and the overall temperature is higher and more uniform. Due to the improved heating capacity, it can be seen from Fig.11 that the mass fraction of hydrogen is larger than that of the original reactor. Besides, the hydrogen concentration is larger, and the progress of the reforming reaction is more sufficient.

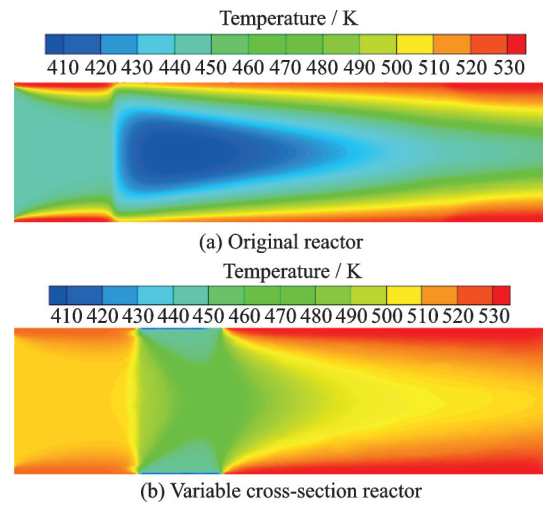


Fig.10 Comparison of temperature distribution of different reactors under the same heating condition

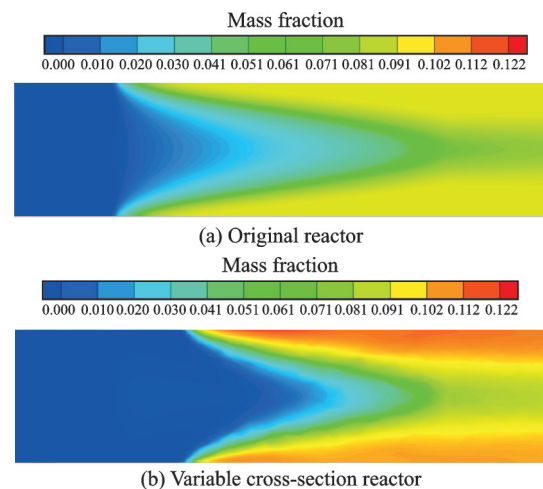


Fig.11 Comparison of different reactors H<sub>2</sub> mass fraction distribution under the same heating condition

Table 7 shows the comparison of reactor performance with different cross-sections at a methanol conversion of about 97% through iterative calcula-

**Table 7 Comparison of boundary temperature and energy consumption**

Scheme	Boundary	Methanol	Energy con-
	temperature/ K	conversion/ %	sumption/ (J·g <sup>-1</sup> )
Original reactor	673	97.02	80.28
Variable cross-section reactor	632	97.04	44.73

tions. It can be seen from Table 7 that with the optimization of the variable cross-section of the reactor, the heating temperature gradually decreases when the same reforming effect is achieved. The heat absorption of the reforming reaction is higher, and the energy consumption per unit of hydrogen production during hot air heating gradually decreases from 80.28 W to 44.73 W, which fully proves the effect of reactor optimization on energy consumption.

### 3 Conclusions

Since the utilization of waste heat in conventional reactors needs to be improved, this paper investigates and designs a variable cross-sectional methanol steam reforming reactor based on the reaction characteristics. Then, based on CFD numerical simulation and response surface methodology, the hydrogen production performance of the new methanol reforming reactor with variable cross-sectional was evaluated and optimized. The main conclusions are as follows:

(1) A low-temperature region at the inlet area of the catalyst bed is formed in the traditional double-jacketed methanol steam reforming reactor due to the strong heat absorption reaction of MSR near the axis and the temperature difference between the lowest temperature of the low-temperature region and the inlet temperature are the largest. In the inlet section of the catalyst bed, the heating demand is greater, so the heating capacity of the front section of the catalyst bed can be increased.

(2) The performance of the reactor can be improved by using a variable cross-sectional heating channel based on the reaction characteristics. The angle of hot air scouring against the wall changes under the obstruction of the tapering cross-sectional, which increases the Reynolds number and thus en-

hances the heat transfer.

(3) The optimal design of the cross-sectional structure by response surface methodology indicates that the reactor performance is optimal for the same heating parameters with  $R_1=49.94$  mm,  $R_2=39.99$  mm and  $D=98.44$  mm.

The design of a new reforming reactor is a key aspect of methanol-reforming for hydrogen production, which is a promising application for onboard hydrogen production due to the increasing interest in hydrogen energy utilization. The results of this study have implications for the development of engine exhaust gas heat reforming for hydrogen production and the optimization of the reactor.

### References

- [1] CHAUBEY R, SAHU S, JAMES O O, et al. A review on development of industrial processes and emerging techniques for production of hydrogen from renewable and sustainable sources[J]. *Renewable & Sustainable Energy Reviews*, 2013, 23(23): 443-462.
- [2] CHOUDHURY A, CHANDRA H, ARORA A. Application of solid oxide fuel cell technology for power generation—A review[J]. *Renewable and Sustainable Energy Reviews*, 2013, 20(4): 430-442.
- [3] LIU Yanyun. Performance study on methanol steam reforming micro-reactor with waste heat recovery[D]. Chongqing: Chongqing University. (in Chinese)
- [4] WANG Jinglin, WANG Haifei, HU P. Theoretical insight into methanol steam reforming on indium oxide with different coordination environments[J]. *Science China: Chemistry*, 2018, 61(3): 336-343.
- [5] WU Sufang. Hydrogen energy and hydrogen producing technologies[M]. Hangzhou: Zhejiang University Press, 2014. (in Chinese)
- [6] LIU Yangxu, ZHOU Wei, LIN Yu, et al. Novel copper foam with ordered hole arrays as catalyst support for methanol steam reforming microreactor[J]. *Applied Energy*, 2019, 246: 24-37.
- [7] RIBEIRINHA P, ABDOLLAHZADEH M, SOUSA J M, et al. Modelling of a high-temperature polymer electrolyte membrane fuel cell integrated with a methanol steam reformer cell[J]. *Applied Energy*, 2017, 202: 6-19.
- [8] MEI Deqing, LIANG Lingwei, QIAN Miao, et al. A performance study of methanol steam reforming in an A-type microchannel reactor[J]. *International Journal of Hydrogen Energy*, 2014, 39(31): 17690-17701.

- [9] SRIVASTAVA A, KUMAR P, DHAR A. A numerical study on methanol steam reforming reactor utilizing engine exhaust heat for hydrogen generation[J]. *International Journal of Hydrogen Energy*, 2021, 46(76): 38073-38088.
- [10] SRIVASTAVA A, KUMAR P, DHAR A. A numerical study on methanol steam reforming reactor utilizing engine exhaust heat for hydrogen generation[J]. *International Journal of Hydrogen Energy*, 2021, 46(76): 38073-38088.
- [11] WANG Longfei. Study on the heat transfer and flow characteristics of novel turbulence generators in gas turbine blades[D]. Harbin: Harbin Institute of Technology. (in Chinese)
- [12] FUKAHORI S, KOGA H, KITAOKA T. Steam reforming behavior of methanol using paper-structured catalysts: Experimental and computational fluid dynamic analysis[J]. *International Journal of Hydrogen Energy*, 2008, 33: 1661-1670.
- [13] LU Weiqing, ZHANG Rongjun, TOAN S, et al. Microchannel structure design for hydrogen supply from methanol steam reforming[J]. *Chemical Engineering Journal*, 2021, 429(27): 132286.

**Acknowledgements** This work was supported by the National Natural Science Foundation of China (No.51806103), the Natural Science Foundation of Jiangsu Province (No.

BK20231445) and the Fundamental Research Funds for the Central Universities (No.501XTCX2023146001).

**Authors** Mr. JIANG Xinyu received the B.S. degree in engineering thermophysics from Jiangsu University in 2021. He is currently a postgraduate student in Nanjing University of Aeronautics and Astronautics. His research is focused on hybrid power system energy and thermal management.

Dr. HE Zhenzong received his Ph.D. degree in engineering thermophysics from Harbin Institute of Technology in 2016. He is currently an associate professor in Nanjing University of Aeronautics and Astronautics. His research is focused on the radiative heat transfer of high gas and soot in the aeroengine combustion chamber, soot size inversion prediction and fuel cell system.

**Author contributions** Mr. JIANG Xinyu contributed to the discussion and analysis. Mr. ZHU Ruihan contributed to the discussion and analysis as well as prepared all drafts, and draw all the figures. Dr. HE Zhenzong and Ms. RAN Qianxi contributed to design of the study and wrote the manuscript. Prof. MAO Junkui contributed to the background, discussion, and analysis of the study. All authors commented on the manuscript draft and approved the submission.

**Competing interests** The authors declare no competing interests.

(Production Editor: ZHANG Huangqun)

## 基于反应特性的可变截面甲醇水蒸气重整反应器优化

蒋新宇<sup>1</sup>, 贺振宗<sup>1,2</sup>, 毛军逵<sup>1</sup>, 朱瑞韩<sup>1</sup>, 冉千禧<sup>1</sup>

(1.南京航空航天大学能源与动力学院,南京 210016,中国; 2.先进航空发动机协同创新中心,北京 100191,中国)

**摘要:**研究了双套管式甲醇水蒸气重整(Methanol steam reforming, MSR)反应器在热空气加热条件下重整通道中的流场特征和催化床的温度分布特性,结果表明:催化床的温度沿流向迅速降低,最低温度在距催化床入口 15 mm 至 20 mm 处;然后,温度随流动方向逐渐升高至反应温度;此外,沿半径方向从中心到壁面催化床温度逐渐升高,热阻的存在使得催化床中心的温度低于周围的温度。根据这一反应特点,本文提出了一种变截面重整反应器,以充分利用供热能量,提高反应效率;然后利用响应面分析法(Response surface methodology, RSM)对变截面反应器的结构参数进行了优化。结果表明,在相同的边界条件下,加热通道重整入口处的外半径 $R_1=49.94$  mm,最小横截面处的半径 $R_2=39.99$  mm,最小横截面到催化床入口的距离 $D=98.44$  mm,甲醇转化率显著提高。

**关键词:**甲醇水蒸气重整;变截面反应器;甲醇转化率;响应面分析法